JACS
JOURNAL OF THE AMERICAN CHEMICAL SOCIETY
Communication
pubs.acs.org/JACS

Zero Thermal Expansion and Ferromagnetism in Cubic $Sc_{1-x}M_xF_3$ (M = Ga, Fe) over a Wide Temperature Range

Lei Hu,[†] Jun Chen,*[,†] Longlong Fan,[†] Yang Ren,[‡] Yangchun Rong,[†] Zhao Pan,[†] Jinxia Deng,[†] Ranbo Yu,[†] and Xianran Xing*[,†]

[†]Department of Physical Chemistry, University of Science and Technology Beijing, Beijing 100083, China
[‡]X-Ray Science Division, Argonne National Laboratory, Argonne, Illinois 60439, United States

Supporting Information

ABSTRACT: The rare physical property of zero thermal expansion (ZTE) is intriguing because neither expansion nor contraction occurs with temperature fluctuations. Most ZTE, however, occurs below room temperature. It is a great challenge to achieve isotropic ZTE at high temperatures. Here we report the unconventional isotropic ZTE in the cubic $(Sc_{1-x}M_x)F_3$ (M = Ga, Fe) over a wide temperature range (linear coefficient of thermal expansion (CTE), $\alpha_l = 2.34 \times 10^{-7}$ K^{-1}, 300−900 K). Such a broad temperature range with a considerably negligible CTE has rarely been documented. The present ZTE property has been designed using the introduction of local distortions in the macroscopic cubic lattice by heterogeneous cation substitution for the Sc site. Even though the macroscopic crystallographic structure of $(Sc_{0.85}Ga_{0.05}Fe_{0.1})F_3$ adheres to the cubic system ($Pm\bar{3}m$) according to the results of X-ray diffraction, the local structure exhibits a slight rhombohedral distortion. This is confirmed by pair distribution function analysis of synchrotron radiation X-ray total scattering. This local distortion may weaken the contribution from the transverse thermal vibration of fluorine atoms to negative thermal expansion, and thus may presumably be responsible for the ZTE. In addition, the present ZTE compounds of $(Sc_{1-x}M_x)F_3$ can be functionalized to exhibit high-T_c ferromagnetism and a narrow-gap semiconductor feature. The present study shows the possibility of obtaining ZTE materials with multifunctionality in future work.

It is well-known that most materials expand on heating. Interestingly, in several cases the property of negative thermal expansion (NTE) has been observed.[1−9] The well-studied origin of NTE in framework materials stems from phonon-related transverse cooperative vibration, such as the rigid polyhedral units in ZrW_2O_8,[1] ScF_3,[2] and geometrically flexible diatomic linkages in $Ag_3[Co(CN)_6]$.[3] Other mechanisms giving rise to NTE include magnetic transition in Invar Fe−Ni alloys[4] and nanocrystalline CuO,[5] spontaneous polarization in $PbTiO_3$-based ferroelectrics,[6,7] and change of electronic configuration in $BiNiO_3$ and $LaCu_3Fe_4O_{12}$.[8,9] The occurrence of NTE in materials provides the possibility to control the rare but much desired property of thermal expansion, which is valuable not only in engineering but also in functional materials, i.e., zero thermal expansion (ZTE), because ZTE materials can be free from the thermally induced stress of thermal fluctuation.[10] However, there are only a few ZTE compounds, like Invar alloys,[4] $Zr_{0.6}Sn_{0.4}Mo_2O_8$,[11] nano $Mn_3Cu_{1-x}Ge_xN$,[12] and $Fe[Co(CN)_6]$.[13] Furthermore, most isotropic ZTE compounds are restricted to a relatively low and narrow temperature range,[14] due to the theoretical fact that low-frequency phonon vibration modes contributing to NTE are preferentially excited at low temperature. With increasing temperature, the relatively high frequency modes can be more dominant, leading to thermal expansion rather than ZTE.[15] It is a great challenge to achieve isotropic ZTE over a wide temperature range.

Here we report an isotropic ZTE over a wide temperature range in ScF_3-based compounds using chemical substitution. The cubic phase of $(Sc_{0.85}Ga_{0.05}Fe_{0.1})F_3$ shows an isotropic ZTE property in a wide temperature range of 300−900 K. Its ZTE behavior is correlated to a local rhombohedral distortion, which probably reduces the phonon transverse vibration. Moreover, the ZTE compound $(Sc_{0.85}Ga_{0.05}Fe_{0.1})F_3$ shows a high-T_c (∼435 K) ferromagnetism and narrow-gap semiconductor feature (band gap of ∼1.88 eV). The present work provides a good example of ZTE materials with multifunctional properties.

At ambient conditions, ScF_3 adopts a cubic ReO_3-tpye structure. It is framework structure and only consists of corner-sharing ScF_6 octahedra. The NTE is proposed to be correlated to the rotary coupling of the fluorine-bridged octahdra rigid units. The distance of Sc···Sc is shortened, resulting in a volumetric contraction on heating.[2] In the present study, we suppose that isotropic ZTE can be achieved by the introduction of local distortion in the macroscopic cubic lattice, which could to some extent reduce the role of phonon transverse vibration to NTE. In this way, we adopt the chemical substitution by isovalent cations of Fe^{3+} and Ga^{3+} for Sc^{3+}. Fe^{3+} (0.645 Å) and Ga^{3+} (0.62 Å) are smaller than that of Sc^{3+} (0.745 Å).[16] The radius differences of Fe^{3+} and Ga^{3+} with respect to the Sc^{3+} cation are 13.4% and 16.8%, respectively. The distortion, arising from the size mismatch of Fe^{3+}, Ga^{3+}, and Sc^{3+} cations, would not be so considerable to result in a phase transition, and thus it will maintain the macroscopic cubic symmetry. In addition, Fe, as a kind of transition element, may introduce magnetism to the spectra of properties in the $(Sc,M)F_3$ system.

Received: July 29, 2014
Published: September 18, 2014

dx.doi.org/10.1021/ja5077487 | J. Am. Chem. Soc. 2014, 136, 13566−13569

A series of ScF_3-based compounds, i.e., $(Sc,M)F_3$ (M = Ga, Fe), were prepared by a solid-state reaction method. In the present study, five compositions—ScF_3, $(Sc_{0.95}Ga_{0.05})F_3$, $(Sc_{0.9}Ga_{0.05}Fe_{0.05})F_3$, $(Sc_{0.85}Ga_{0.05}Fe_{0.1})F_3$, and $(Sc_{0.8}Ga_{0.05}Fe_{0.15})F_3$—were prepared. All five compositions remain in the cubic crystal symmetry according to X-ray diffraction (XRD) investigations (Figure S1). Details on sample preparation, high-temperature XRD, magnetic characterization, UV−vis spectra, and synchrotron radiation X-ray total scattering PDF analyses are provided in the Supporting Information. By systematic substitution for the Sc^{3+} cation, the NTE of each of these $(Sc,M)F_3$ (M = Ga, Fe) compounds has been weakened to different degrees, while the crystal structure remains in cubic symmetry at all investigated temperatures from 300 to 900 K. ScF_3 shows a strong and smooth NTE behavior with a linear CTE of $\alpha_l = -3.1 \times 10^{-6}$ K^{-1} (300−900 K). This value is consistent with the value of $\alpha_l = -3.0 \times 10^{-6}$ K^{-1} reported in the literature.[2] After the substitution of only 5 mol% Ga^{3+} for Sc^{3+}, the NTE of $(Sc_{0.95}Ga_{0.05})F_3$ is slightly weakened ($\alpha_l = -2.4 \times 10^{-6}$ K^{-1}, 300−900 K). After the co-substitution by both Ga^{3+} and Fe^{3+} for Sc^{3+}, the NTE property of $(Sc_{0.9}Ga_{0.05}Fe_{0.05})F_3$ is considerably impeded with a small CTE ($\alpha_l = -1.3 \times 10^{-6}$ K^{-1}, 300−900 K). Positive thermal expansion (PTE) has been achieved in $(Sc_{0.8}Ga_{0.05}Fe_{0.15})F_3$ ($\alpha_l = 3.3 \times 10^{-6}$ K^{-1}, 300−900 K). The XRD patterns collected at 300 K and temperature evolution of lattice constants of ScF_3, $(Sc_{0.95}Ga_{0.05})F_3$, $(Sc_{0.9}Ga_{0.05}Fe_{0.05})F_3$, and $(Sc_{0.8}Ga_{0.05}Fe_{0.15})F_3$ are presented in Figure S1 and Table S2. Interestingly, the ZTE property is achieved in the composition of $(Sc_{0.85}Ga_{0.05}Fe_{0.1})F_3$ (the effective composition investigated by inductively coupled plasma mass spectrometry (ICP-MS): $(Sc_{0.82}Ga_{0.06}Fe_{0.12})F_3$), where the lattice constant remains nearly constant throughout a considerably wide temperature range from 300 to 900 K (Figure 1). The value of CTE ($\alpha_l = 2.3 \times 10^{-7}$ K^{-1}) is

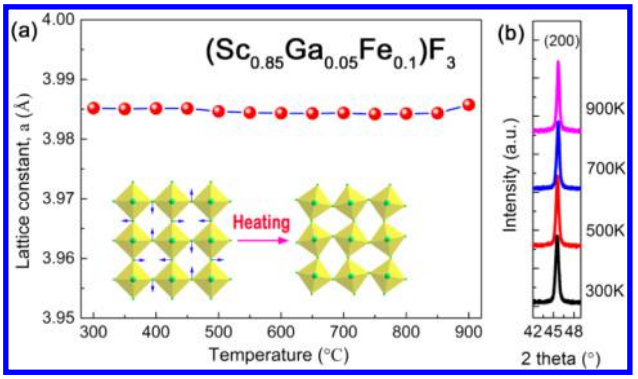

Figure 1. (a) Temperature evolution of lattice constant of $(Sc_{0.85}Ga_{0.05}Fe_{0.1})F_3$. The inset shows the cooperative vibration of rigid ScF_6 octahedra on heating. Blue arrows indicate the transverse vibration of fluorine atoms. (b) (200) peak of XRD patterns at different temperatures of $(Sc_{0.85}Ga_{0.05}Fe_{0.1})F_3$.

minuscule, highlighting the nature of ZTE behavior. As shown in Figure 1b, direct visual inspection of the XRD pattern further verifies the ZTE property. With increasing temperature, the (200) peak of $(Sc_{0.85}Ga_{0.05}Fe_{0.1})F_3$ does not shift evidently. In comparison, the thermal expansion properties for representative ZTE materials are summarized (Table S4). It should be noted that most ZTE compounds exhibit the ZTE property over a narrow temperature range, except for $Zr_{0.4}Sn_{0.6}Mo_2O_8$,[11] and normally at low temperatures. The ZTE in the present composition of $(Sc_{0.85}Ga_{0.05}Fe_{0.1})F_3$ can be extended to much higher temperatures. Such a wide ZTE temperature range is exceptional, since thermal vibration of the lattice should be large at such high temperatures.

In addition to the intriguing ZTE behavior, a high-T_c ferromagnetic loop and deduction of a large linear contribution have also been observed in $(Sc_{0.85}Ga_{0.05}Fe_{0.1})F_3$. For those compositions without Fe, ScF_3 and $(Sc_{0.95}Ga_{0.05})F_3$ show diamagnetic behavior (Figure S3), since Sc^{3+} and Ga^{3+} have the $3d^0$ and $3d^{10}$ electron configurations, respectively. When Fe atoms are incorporated, $(Sc_{0.85}Ga_{0.05}Fe_{0.1})F_3$ clearly demonstrates a magnetic hysteretic phenomenon (Figure 2). This

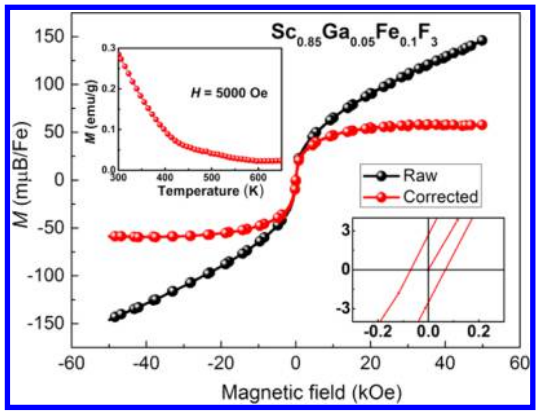

Figure 2. $M-H$ curve of $(Sc_{0.85}Ga_{0.05}Fe_{0.1})F_3$, measured in the external magnetic field up to 50 kOe at room temperature, exhibiting the initial magnetic loop and deduction of a large linear contribution. The inset at the top-left shows its $M-T$ curve in H = 5000 Oe and the inset at the bottom-right displays H_c in the low magnetic region. The diamagnetic sign of the sample holder has been subtracted.

indicates a robust ferromagnetic behavior with a coercivity of ∼70 Oe (inset at the bottom right of Figure 2). The $M-H$ curve is associated with a large linear component, presumably due to remaining paramagnetic spins.[17]

Temperature dependence of magnetization in an external field of ∼5000 Oe was also investigated for $(Sc_{0.8}Ga_{0.05}Fe_{0.15})F_3$. On heating, the magnetic moment decreases slowly and demonstrates a broader magnetic transition temperature span, leading to a T_c as high as ∼435 K. The corresponding reciprocal susceptibility ($1/\chi$) as a function of temperature was also depicted in Figure S3d. Compared to other ZTE materials displaying magnetism, where magnetism commonly works below room temperature, it is interesting to observe such high-T_c ferromagnetism in the present ZTE composition of $(Sc_{0.85}Ga_{0.05}Fe_{0.1})F_3$. Considerable band gap narrowing also occurs in $(Sc_{0.85}Ga_{0.05}Fe_{0.1})F_3$ with a noticeable visible-light absorption and band gap value of ∼1.88 eV (Figure S4), compared to the insulator ScF_3 (5.5−6.0 eV).[18] New emerging impurity energy levels, mainly composed of Fe 3d and F 2p states around the Fermi level, are presumably responsible for the large reduction in band gap.

What is the mechanism for the ZTE in $(Sc_{0.85}Ga_{0.05}Fe_{0.1})F_3$? There could exist local distortions in $(Sc,M)F_6$ (M = Ga and Fe) which are responsible for the mechanism of ZTE, even though it is in macroscopic cubic symmetry as shown by the XRD investigation. In order to investigate the local structure, we carried out atomic pair distribution function (PDF) analysis of synchrotron radiation X-ray total scattering for undoped

dx.doi.org/10.1021/ja5077487 | J. Am. Chem. Soc. 2014, 136, 13566−13569

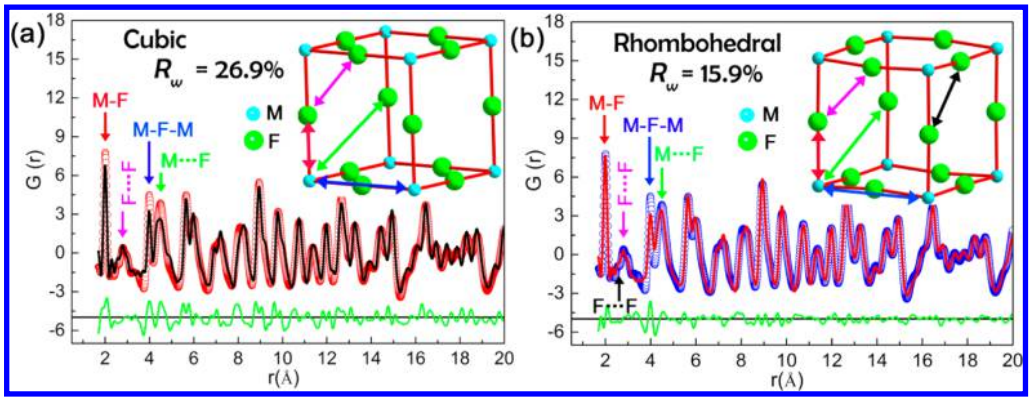

Figure 3. Pair distribution function (PDF) fit of synchrotron radiation X-ray total scattering obtained at 300 K for the $(Sc_{0.85}Ga_{0.05}Fe_{0.1})F_3$ with (a) the cubic model and (b) the rhombohedral model at low r (1.7−20 Å). The red and blue circles correspond to the experimental data. Black and red lines represent the calculated data. Difference curves are shown by green lines. The cubic and rhombohedral models are depicted in the top right corners of panels a and b, respectively. PDF peaks labeled by different color arrows correspond to different atom pairs marked by the same color double-headed arrows. M here indicates Sc, Ga, and Fe.

ScF_3, $(Sc_{0.9}Ga_{0.05}Fe_{0.05})F_3$, and $(Sc_{0.85}Ga_{0.05}Fe_{0.1})F_3$. Initially, the cubic $Pm\bar{3}m$ model was adopted (inset in Figure 3a), in accordance with the XRD result, to analyze the local structure of $(Sc_{0.85}Ga_{0.05}Fe_{0.1})F_3$.

However, the cubic model cannot be reconciled with the experimental PDF data (Figure 3a), as demonstrated by the high value of agreement factor (R_w = 26.9%). It can be expected that with the substitution of different size atoms for the Sc site, distortion would inevitably appear at a local scale. It is known that representative ReO_3-type metal trifluorides with lattice disorder commonly remain in $R\bar{3}c$ symmetry, such as AlF_3.[19] Thus, the rhombohedral mode ($R\bar{3}c$) was used to describe the possible local structure for $(Sc_{0.85}Ga_{0.05}Fe_{0.1})F_3$. Refinement based on the $R\bar{3}c$ model yields a considerably improved fit to the experimental data (R_w = 15.9%, shown in Figure 3b). It is especially superior in modeling the nearest neighboring M−F and the next-nearest neighboring M···F PDF peaks, although some discrepancies still remain, such as the peak positioned at 3.98 Å. The rhombohedral model is presented in a *cubic-like* form rather than the form of rhombohedral unit cell (inset of Figure 3b). The special form was extracted from the rhombohedral structure (Figure S5). The difference between the cubic model and the rhombohedral one is discussed below.

Given that an experimental PDF can be treated as the assembly of snapshots of the instantaneous atomic arrangements, low and high r corresponds to low structure and average structure, respectively. The high-r (from 20 to 60 Å) experimental PDF of $(Sc_{0.85}Ga_{0.05}Fe_{0.1})F_3$ was also refined (Figure S7). A closer inspection of the high-r experimental data, however, demonstrates that the cubic model outperforms the rhombohedral one. This indicates that the long-range structure of $(Sc_{0.85}Ga_{0.05}Fe_{0.1})F_3$ is cubic, which is consistent with the Rietveld refinement result (Figure S1 and Table S2). The high-r PDF result demonstrates that the design of co-substitution by Fe^{3+} and Ga^{3+} is appropriate to retain the macroscopic cubic structure. If the difference in ionic radii is considerably large, such as in $(Sc_{1-x}Y_x)F_3$ (the difference of Y^{3+} and Sc^{3+} ion radii reaches 21%),[20] it would inevitably result in considerable lattice distortion and a cubic-to-rhombohedral phase transition.

PDF analyses demonstrate that the rhombohedral model is superior to the cubic counterpart at low r in $(Sc_{0.85}Ga_{0.05}Fe_{0.1})F_3$. However, this situation is opposite when it comes to the higher r. In short, it confirms the coexistence of a lower symmetry in the local atomic arrangements and a higher symmetry average structure. This situation is not unusual, as it has ever been observed in crystalline materials such as In−Ga−As semiconductors.[21] In contrast, PDF analysis in the undoped ScF_3, displays that, at low r, the cubic model provides a better fit to the experimental data than the rhombohedral model (Figure S8). The distinction of local structures in ScF_3 and $(Sc_{0.85}Ga_{0.05}Fe_{0.1})F_3$ is presumably correlated with their different behaviors of thermal expansion.

Deviating from the ideal cubic structure, local atomic arrangements of $(Sc_{0.85}Ga_{0.05}Fe_{0.1})F_3$ are subjected to rhombohedral distortion. Figure 4a,b clearly exhibits the two different

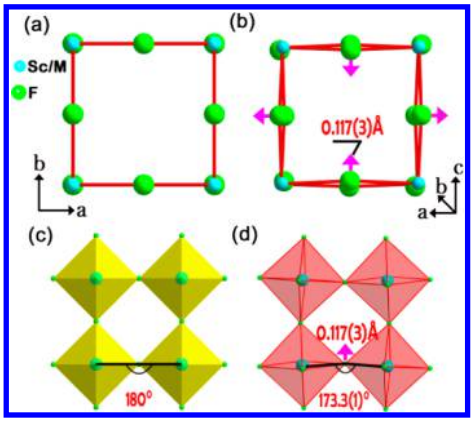

Figure 4. (a) The cubic model. (b) The rhombohedral model in *cubic-like* form with purple arrows indicating static displacement of fluorine atoms. (c) Ideal stacking $(Sc,M)F_6$ octahedrons in the cubic model with the 180° angle of Sc/M−F−Sc/M. (d) Distorted stacking $(Sc,M)F_6$ octahedrons in the rhombohedral model with the 173.3(1)° angle of Sc/M−F−Sc/M.

local structures. In the cubic model, fluorine atoms locate exactly at the midpoint of the Sc/M−F−Sc/M linkage and Sc/M−F−Sc/M angles remain at 180° (Figure 4c). As for the distorted model, fluorine atoms depart from the original midpoint with a displacement of 0.117(3) Å shown by the purple arrows (for details see Figure S9), associated with the bending Sc/M−F−Sc/M linkage (Figure 4b). The distorted stacking octahedral give the Sc/M−F−Sc/M angle of ∼173.3(1)° (Figure 4d). It is presumed that this local

dx.doi.org/10.1021/ja5077487 | J. Am. Chem. Soc. 2014, 136, 13566−13569

rhombohedral structure has a strong correlation with the ZTE behavior in $(Sc_{0.85}Ga_{0.05}Fe_{0.1})F_3$. As reported previously,[2] ScF_3 adopts the cubic ReO_3 structure with straight Sc−F−Sc linkages.

Upon heating, the transverse vibration of F anion normal to the straight Sc···Sc axis, involving the cooperative rotation of ScF_6 octahedra rigid units, gives rise to a reduction in Sc···Sc separations and thus ensures strong NTE. In the present ZTE material of $(Sc_{0.85}Ga_{0.05}Fe_{0.1})F_3$, at the *B*-site 15 mol% Sc^{3+} is replaced by heterogeneous cations of Ga^{3+}/Fe^{3+}. Its local structure is rhombohedrally distorted with bending M−F−M linkages, which could impede the cooperative rotation of $(Sc,M)F_6$ octahedra rigid units and thus weaken the NTE. Eventually, when NTE is dampened to a certain extent, ZTE occurs, and here it occurs in the composition of $(Sc_{0.85}Ga_{0.05}Fe_{0.1})F_3$. As a comparison, most ReO_3-type metal trifluorides, such as AlF_3 and TiF_3, generally show macroscopic distortion of rhombohedral symmetry (space group $R\bar{3}c$), featuring larger bending of M−F−M linkages (Al−F−Al ≈ 157.6°, Ti−F−Ti ≈ 160.8°).[19,22] They do not exhibit NTE but normal PTE. Therefore, it could be inferred that the ZTE of $(Sc_{0.85}Ga_{0.05}Fe_{0.1})F_3$ is highly correlated with local distortions and bending of M−F−M linkages.

For NTE compounds with open framework structure, the present study provides a possible approach to mediate NTE to the desirable ZTE property, by the introduction of slight local distortion, arising from the substitution of heterogeneous cations. In addition, it also could achieve multifunctionality, like applications in magnetic−optical switching or magnetic semiconductors,[23] in ZTE compounds.

In summary, isotropic ZTE has been observed in cubic $(Sc_{0.85}Ga_{0.05}Fe0.1)F_3$ over a wide temperature range (300−900 K). It is unconventional to observe the isotropic ZTE over such wide temperature range. PDF analysis provides an insight into the local structure. The local rhombohedra structure features a slightly bending Sc/M−F−Sc/M linkage. The static displacement of fluorine from the axis of Sc/M···Sc/M reaches 0.117(3) Å. This local distortion may impede the transverse vibration of rigid $(Sc,M)F_6$ octahedra and thus is presumably responsible for the ZTE property. Furthermore, the present ZTE $(Sc_{0.85}Ga_{0.05}Fe_{0.1})F_3$ exhibits high-temperature ferromagnetism (T_c ≈ 435 K) and narrow band gap semiconductor characteristics. The enormous diversities in structure, magnetism, and electronic properties of $(Sc,M)F_3$ (M = Ga, Fe) can be referred to for further exploration to design other controllable NTE or ZTE materials with multifunctional properties.

■ ASSOCIATED CONTENT

Ⓢ Supporting Information

Details of lattice constants, anisotropic displacement parameters, PDF analyses, and other correlated information. This material is available free of charge via the Internet at http://pubs.acs.org.

■ AUTHOR INFORMATION

Corresponding Authors

junchen@ustb.edu.cn
xing@ustb.edu.cn

Notes

The authors declare no competing financial interest.

■ ACKNOWLEDGMENTS

This work was supported by National Natural Science Foundation of China (Grant Nos. 21322102, 21031005, 21231001), Program for Changjiang Scholars and Innovative Research Team in University (IRT1207). Use of the Advanced Photon Source, an Office of Science User Facility operated for the U.S. Department of Energy (DOE) Office of Science by Argonne National Laboratory, was supported by the U.S. DOE under Contract No. DE-AC02-06CH11357.

■ REFERENCES

(1) Mary, T.; Evans, J.; Vogt, T.; Sleight, A. *Science* **1996**, *272*, 90.
(2) Greve, B. K.; Martin, K. L.; Lee, P. L.; Chupas, P. J.; Chapman, K. W.; Wilkinson, A. P. *J. Am. Chem. Soc.* **2010**, *132*, 15496.
(3) Goodwin, A. L.; Calleja, M.; Conterio, M. J.; Dove, M. T.; Evans, J. S.; Keen, D. A.; Peters, L.; Tucker, M. G. *Science* **2008**, *319*, 794.
(4) Mohn, P. *Nature* **1999**, *400*, 18.
(5) Zheng, X.; Kubozono, H.; Yamada, H.; Kato, K.; Ishiwata, Y.; Xu, C. *Nat. Nanotechnol.* **2008**, *3*, 724.
(6) Chen, J.; Nittala, K.; Forrester, J. S.; Jones, J. L.; Deng, J.; Yu, R.; Xing, X. *J. Am. Chem. Soc.* **2011**, *133*, 11114.
(7) Chen, J.; Fan, L.; Ren, Y.; Pan, Z.; Deng, J.; Yu, R.; Xing, X. *Phys. Rev. Lett.* **2013**, *110*, No. 115901.
(8) Azuma, M.; Chen, W.-t.; Seki, H.; Czapski, M.; Oka, K.; Mizumaki, M.; Watanuki, T.; Ishimatsu, N.; Kawamura, N.; Ishiwata, S. *Nat. Commun.* **2011**, *2*, 347.
(9) Long, Y.; Hayashi, N.; Saito, T.; Azuma, M.; Muranaka, S.; Shimakawa, Y. *Nature* **2009**, *458*, 60.
(10) Sleight, A. *Nature* **2003**, *425*, 674.
(11) Tallentire, S. E.; Child, F.; Fall, I.; Vella-Zarb, L.; Evans, I. R.; Tucker, M. G.; Keen, D. A.; Wilson, C.; Evans, J. S. *J. Am. Chem. Soc.* **2013**, *135*, 12849.
(12) Song, X.; Sun, Z.; Huang, Q.; Rettenmayr, M.; Liu, X.; Seyring, M.; Li, G.; Rao, G.; Yin, F. *Adv. Mater.* **2011**, *23*, 4690.
(13) Margadonna, S.; Prassides, K.; Fitch, A. N. *J. Am. Chem. Soc.* **2004**, *126*, 15390.
(14) Roy, R.; Agrawal, D. K.; McKinstry, H. A. *Annu. Rev. Mater. Sci.* **1989**, *19*, 59.
(15) Wang, L.; Yuan, P.-F.; Wang, F.; Sun, Q.; Liang, E.-J.; Jia, Y. *Mater. Res. Bull.* **2012**, *47*, 1113.
(16) Shannon, R. T. *Acta Crystallogr. Sect. A: Cryst. Phys., Diffr., Theor. Gen. Crystallogr.* **1976**, *32*, 751.
(17) Zhao, K.; Deng, Z.; Wang, X.; Han, W.; Zhu, J.; Li, X.; Liu, Q.; Yu, R.; Goko, T.; Frandsen, B. *Nat. Commun.* **2013**, *4*, 1442.
(18) Zhgun, P.; Bocharov, D.; Piskunov, S.; Kuzmin, A.; Purans, J. *arXiv* **2012**, No. arXiv:1211.5697.
(19) Chupas, P. J.; Chaudhuri, S.; Hanson, J. C.; Qiu, X.; Lee, P. L.; Shastri, S. D.; Billinge, S. J.; Grey, C. P. *J. Am. Chem. Soc.* **2004**, *126*, 4756.
(20) Morelock, C. R.; Greve, B. K.; Gallington, L. C.; Chapman, K. W.; Wilkinson, A. P. *J. Appl. Phys.* **2013**, *114*, No. 213501.
(21) Petkov, V.; Jeong, I.; Chung, J.; Thorpe, M.; Kycia, S.; Billinge, S. *Phys. Rev. Lett.* **1999**, *83*, 4089.
(22) Kennedy, B. J.; Vogt, T. *Mater. Res. Bull.* **2002**, *37*, 77.
(23) Goodwin, A. L. *Nat. Nanotechnol.* **2008**, *3*, 710.